

Phase transitions and regions of stability in Reissner-Nordström holographic superconductors.

E. Abdalla^{a,*} C. E. Pellicer^{a,†} and Jeferson de Oliveira^{a‡}

^a*Instituto de Física, Universidade de São Paulo,
CP 66318, 05315-970, São Paulo, Brazil*

A. B. Pavan^{b§}

^b*Instituto de Ciências Exatas, Universidade Federal de Itajubá,
Av. BPS 1303 Pinheirinho, 37500-903 Itajubá, MG, Brazil*

Abstract

The phase transition of Reissner-Nordström AdS_4 interacting with a massive charged scalar field has been further revisited. We found exactly one stable and one unstable quasinormal mode regions for the scalar field. The two of them are separated by the first marginally stable solution.

PACS numbers: 04.70.Bw, 11.25.Tq, 74.20.-z

*Electronic address: eabdalla@usp.br

†Electronic address: carlosep@fma.if.usp.br

‡Electronic address: jeferson@fma.if.usp.br

§Electronic address: alan@unifei.edu.br

The AdS/CFT correspondence [1] has been used as a very important tool to probe physics beyond the usual application in string theory, namely quark gluon plasma, fluid mechanics as well as condensed matter models [2–5]. In the present discussion we analyse a model first considered in [4] and later by many authors [5–10] related to superconductors and corresponding phase transitions, generally referred to as holographic superconductors.

The AdS/CFT correspondence relates the gravitational fields in a bulk to properties of a field theory at its border. Moreover, the weak coupling in one of the counterparts becomes the strong coupling limit of the other. In [4, 11] a break of the $U(1)$ gauge symmetry has been achieved by a charged scalar interacting with a black hole in the bulk, a mechanism leading, eventually, to a superconductor at the boundary — what has been called a holographic superconductor. Several similar mechanisms have been proposed in the literature. In particular, it has been shown that several phase transitions may occur in a given model [4]. Such a conclusion has been formulated upon computing the perturbations in the bulk and looking for the time independent perturbations, which presumably divide sectors of growing and decaying modes.

Here we show that there are just two sectors, namely a superconducting and a normal phase, in view of the fact that even beyond the marginally stable solution growing modes still exist. Such a result comes about from the existence of further unstable modes, which we were able to compute explicitly by the Quasi Normal Modes technique [12].

We consider the bulk action of a massive charged scalar field ψ interacting with an Abelian field A_μ generated by a charged AdS black hole. The Lagrange density is that of Einstein gravity with a cosmological constant, a charged scalar and a gauge field, that is,

$$16\pi G\mathcal{L} = R + \frac{6}{L^2} - \frac{F_{\mu\nu}^2}{4} - |\partial_\mu\psi - iqA_\mu\psi|^2 - m^2|\psi|^2 \quad . \quad (1)$$

The above Lagrangian has also been used in [4] in the same context. The background spacetime is a spherically symmetric Reissner-Nordström AdS_4 , that is,

$$ds^2 = -f(r) dt^2 + \frac{1}{f(r)} dr^2 + r^2 d\Omega_2^2 \quad , \quad (2)$$

with

$$f(r) = 1 - \frac{2M}{r} + \frac{Q^2}{4r^2} + \frac{r^2}{L^2} \quad , \quad (3)$$

where Q and M are respectively the electric charge and mass of the black hole. Besides, L refers to the AdS radius, which is related to the cosmological constant Λ by $L = \sqrt{-3/\Lambda}$.

The Hawking temperature of this black hole is given by

$$T = \frac{1}{4\pi} \left[\frac{4r_+^2 - Q^2}{4r_+^3} + \frac{3r_+}{L^2} \right] . \quad (4)$$

One identifies the parameters of the black hole with a critical temperature T_* that characterizes the phase transition. In [13], this T_* can be related to the critical temperature T_c of a holographic superconductor.

The solution for the gauge field A_μ reads

$$A_\mu dx^\mu = \Phi(r) dt \quad , \quad (5)$$

where the electric potential is written in terms of black hole charge Q and the position of event horizon r_+ as

$$\Phi = \frac{Q}{r} - \frac{Q}{r_+} . \quad (6)$$

For our purposes, we assume that the scalar field ψ is a small perturbation that does not backreact. In this regime, we can use the quasinormal modes techniques in order to compute the ψ -propagation. Its equation of motion results in

$$D_\mu D^\mu \psi = m^2 \psi \quad , \quad (7)$$

where $D_\mu = \nabla_\mu - iqA_\mu$. The parameters m and q are the mass and charge of the scalar field, respectively. Expanding Eq.(7) we find

$$\square\psi - 2iqA_\mu g^{\mu\nu} \partial_\nu \psi - q^2 A_\mu A^\mu \psi - m^2 \psi = 0 \quad . \quad (8)$$

The s-wave mode ($l = 0$ mode in the angular momentum expansion) is easily obtained. For our purposes it is sufficient since higher angular momentum modes are connected with higher decay modes, and we only need the first unstable mode to install instability, as we are going to argue more generally. We follow [4] and set $r_+ = Q = 1$ and our parameters are m , q and L . We find

$$-\frac{\partial^2 \psi}{\partial t^2} + f^2 \frac{\partial^2 \psi}{\partial r^2} + \frac{\partial \psi}{\partial r} \left[\frac{2f^2}{r} + f \frac{df}{dr} \right] + 2iq\Phi \frac{\partial \psi}{\partial t} + q^2 \Phi^2 \psi - m^2 f \psi = 0 \quad . \quad (9)$$

We use the tortoise coordinate $dr_* = \frac{dr}{f}$ and the *Ansatz* $\psi = \frac{\Psi}{r}$ for the field, resulting in the equation

$$-\frac{\partial^2 \Psi}{\partial t^2} + \frac{\partial^2 \Psi}{\partial r_*^2} + 2iq\Phi \frac{\partial \Psi}{\partial t} - V(r)\Psi = 0 \quad , \quad (10)$$

with

$$V(r) = f(r) \left[\frac{f'}{r} + m^2 \right] - q^2 \Phi^2(r) \quad . \quad (11)$$

An analysis of Eq.(10) shows that the procedure used in [14] to discretize the spacetime and integrate the equation of motion is not convenient because of the presence of the term $2iq\Phi \frac{\partial \Psi}{\partial t}$. The method used in the mentioned work normally has numerical error proportional to Δ^4 , where Δ is the step used, but the extra term has an error proportional to Δ^2 , so we used the finite difference method, whose error is proportional to Δ^2 without the need of another coordinate change.

Finite difference method

We define $\Psi(r_*, t) = \Psi(-j\Delta r_*, l\Delta t) = \Psi_{j,l}$, $V(r(r_*)) = V(-j\Delta r_*) = V_j$ and $\Phi(r(r_*)) = \Phi(-j\Delta r_*) = \Phi_j$ to rewrite equation (10) as

$$\begin{aligned} & - \frac{(\Psi_{j,l+1} - 2\Psi_{j,l} + \Psi_{j,l-1})}{\Delta t^2} + 2iq\Phi_j \frac{\Psi_{j,l+1} - \Psi_{j,l-1}}{2\Delta t} \\ & + \frac{(\Psi_{j+1,l} - 2\Psi_{j,l} + \Psi_{j-1,l})}{\Delta r_*^2} - V_j \Psi_{j,l} + O(\Delta t^2) + O(\Delta r_*^2) = 0 \quad . \end{aligned} \quad (12)$$

With a Gaussian distribution with finite support as initial condition and Dirichlet conditions at $r_* = 0$, we derive the evolution of Ψ by

$$\begin{aligned} \Psi_{j,l+1} = (1 - iq\Phi_j \Delta t)^{-1} & \left[- (1 + iq\Phi_j \Delta t) \Psi_{j,l-1} + \frac{\Delta t^2}{\Delta r_*^2} (\Psi_{j+1,l} + \Psi_{j-1,l}) + \right. \\ & \left. + \left(2 - 2\frac{\Delta t^2}{\Delta r_*^2} - \Delta t^2 V_j \right) \Psi_{j,l} \right] \quad . \end{aligned} \quad (13)$$

The Von Neumann stability conditions usually require that $\frac{\Delta t}{\Delta r_*} < 1$. If the effective potential Eq. (11) is too large, the method is unstable even for small Δt . In a simple wave equation $\ddot{x} + \omega^2 x = 0$, this requirement means that the step Δt must be smaller than ω^{-1} . In our case, $V(r)$ is proportional to $\frac{r^2}{L^4} (2 + m^2 L^2)$ for large r (i.e. r_* close to 0), and for $m^2 L^2 = 4$ we can see that even with ratios as low as $\frac{\Delta t}{\Delta r_*} = 0.7$ the method becomes unstable, so we used $\frac{\Delta t}{\Delta r_*} = 0.5$. Therefore, in this work the stability conditions depend on the parameters m and L .

Horowitz-Hubeny method

Another method to find quasinormal modes in asymptotically *AdS* spacetimes was developed by Horowitz and Hubeny [15] and used in [16, 17].

Rewriting the metric Eq.(2) and the gauge field Eq.(5) in terms of ingoing Eddington-Finkelstein coordinate, $v = t + r_*$, results in

$$ds^2 = -f(r) dv^2 + 2 dv dr + r^2 d\Omega_2^2, \quad A_v dv = \Phi(r) dv \quad . \quad (14)$$

In the new coordinates and after performing the separation of variables $\psi(v, r, \theta, \phi) = \frac{Z(r)}{r} Y_{lm}(\theta, \phi) e^{-i\omega v}$ the wave equation Eq.(9) reads

$$f \frac{d^2 Z}{dr^2} + [f' - 2i(\omega + q\Phi)] \frac{dZ}{dr} - V(r) Z = 0 \quad , \quad (15)$$

where the potential is

$$V(r) = \left(m^2 + \frac{f'}{r} - \frac{2iq\Phi}{r} + \frac{\ell(\ell+1)}{r^2} \right) \quad . \quad (16)$$

Following the procedure outlined by Horowitz and Hubeny [15], it is convenient to rewrite the wave equation (15) as

$$s(x) \frac{d^2 Z}{dx^2} + \frac{t(x)}{(x-x_+)} \frac{dZ}{dx} + \frac{u(x)}{(x-x_+)^2} Z = 0 \quad , \quad (17)$$

where we were able to put the functions $s(x)$, $t(x)$ and $u(x)$ in a polynomial form

$$s(x) = x^2 A_0 \quad , \quad (18)$$

$$t(x) = \left\{ 2(x-x_+)x A_0 + x A_1 + 2ix^2 [\omega + q(x-x_+)] \right\} \quad , \quad (19)$$

$$u(x) = (x-x_+) \left\{ A_1 - m^2 + 2iq(x-x_+)x \right\} \quad , \quad (20)$$

with

$$A_0 = \left[\frac{x^3}{4} - \frac{kx^2}{x_+} - \frac{x^2 + x_+x + x_+^2}{L^2 x_+^3} \right] , \quad (21)$$

$$A_1 = \left[-\frac{kx^3}{x_+} + \frac{(2x-x_+)}{4} - \frac{(x^3 + 2x_+^3)}{L^2 x_+^3} \right] . \quad (22)$$

where we set $l = 0$ and $Q = 1$.

Expanding the solution $Z(x)$ to the wave equation (17) around the event horizon $x_+ = 1/r_+$, we have

$$Z(x) = \sum_{n=0}^{\infty} a_n(\omega)(x-x_+)^n. \quad (23)$$

The key point is to compute de roots of the equation $Z(x=0) = 0$ following from the boundary condition at spatial infinity. Actually, we have to truncate the de sum at an

intermediate $n = N$ and check that for the greater n in which the root converge. We compute the zeros ω of $\sum_{n=0}^{\infty} a_n(\omega)(-x_+)^n$ using the software *Mathematica* and also the routine *zroots* [18].

Discussion and Results

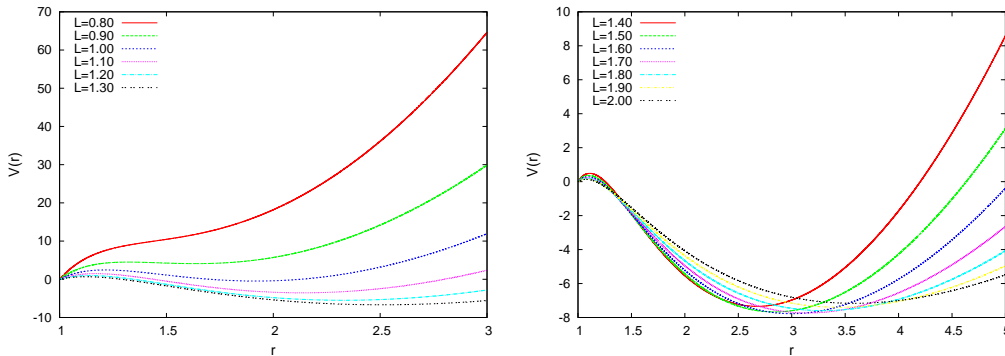


Figure 1: Behavior of effective potential for several values of L (color online).

In Figure (1) we plot the effective potential (11) due to the charged scalar field propagation in the geometry (2) since the stable region, passing through the transition point next to $L = 1.28$ into the unstable region. We clearly see that the potential defines a positive definite barrier near the event horizon ($r_+ = 1$) and becomes negative at intermediate values of radial coordinate diverging at spatial infinite as expected for asymptotically AdS spacetimes. Since we have an additional term in Eq.(10), the result from [15] that a positive definite potential implies stability is not necessarily valid. However, modes with positive definite potentials are stable in this work. Besides, the first unstable mode is presumably related to the first value of L (or highest value of T) whose potential admits a bound state with negative energy.

Figure (2) shows five different behaviors of $\psi(r_*, t)$ given by Eq.(13) at $r_* = -5$ for $m^2 L^2 = 4$ and $qL = 10$. The results show an interesting phenomena. At a value next to $L = 1.28$ we have a phase transition. This is the same transition obtained by Gubser. Our results agree with those, that is, beyond this value of L the black hole become unstable.

Fitting $\Psi = A \exp(\omega_i t) \cos(\omega_r t + \delta)$, we get the quasinormal frequencies. We cannot tell the sign of ω_r using this fitting, but if we assume that ω_r depends smoothly on L , a sign change would appear as a discontinuity in the first derivative, as our data appears. Choosing

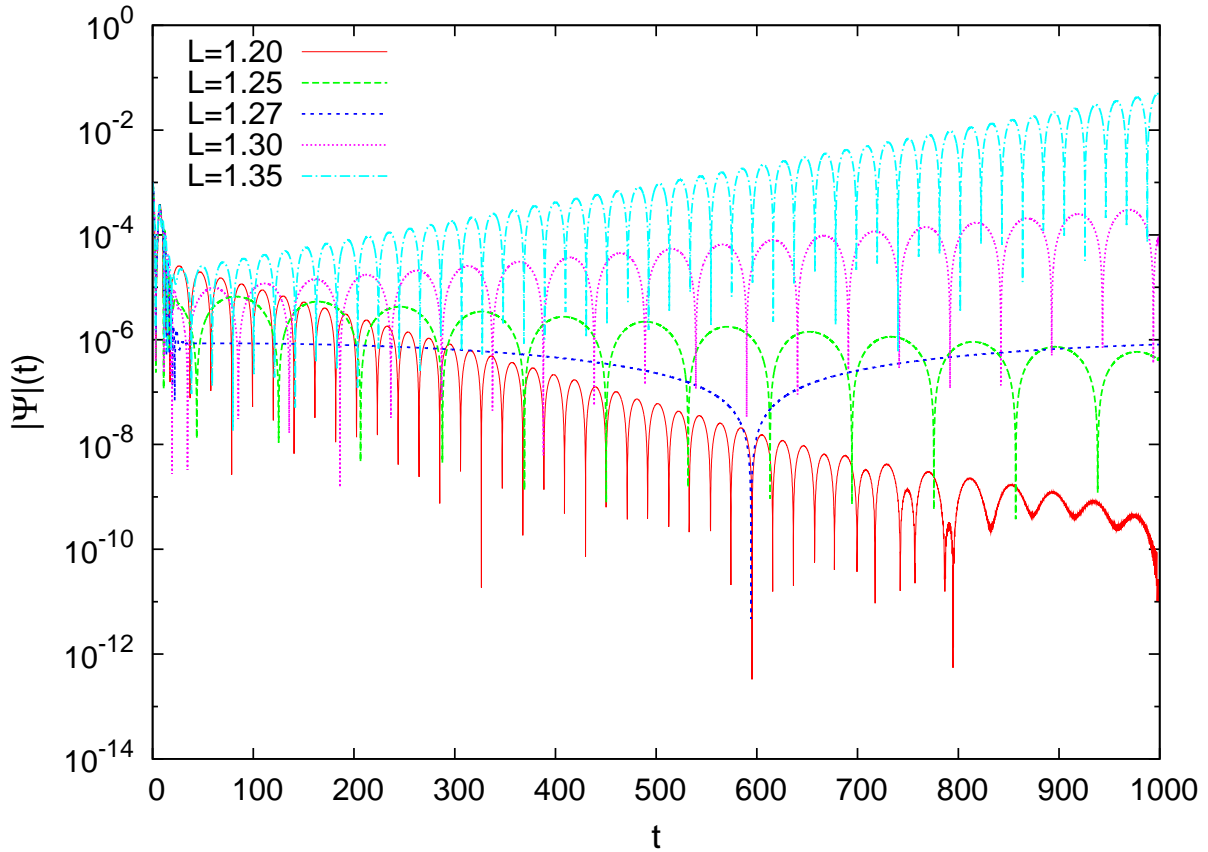


Figure 2: Quasinormal modes versus t (color online).

the sign of ω_r as the same of ω_i , we obtain the figure (3), which shows that both ω_r and ω_i change sign at the same value of L . In the same figure we adjust the scale so that the sign change is clearly seen. We are also interested in the dependence of these frequencies with the temperature, shown in figure (4), in this figure we also adjust the scale to better see the transition. We noticed that the transition occurs at a value of L smaller than expected in [4]. Since the numerical method used to solve second order partial differential equations has errors larger than methods commonly used to solve second order ordinary differential equations, we believe that this difference is due to numerical errors.

There are further secondary quasinormal modes. We found the next one which is presented in figure (5). Indeed, the secondary mode shows a zero frequency at L next to the second marginally stable mode found in [4]. However, the first mode remains, and it is unstable. This means that the model remains unstable and superconductivity still holds beyond that second marginally stable mode.

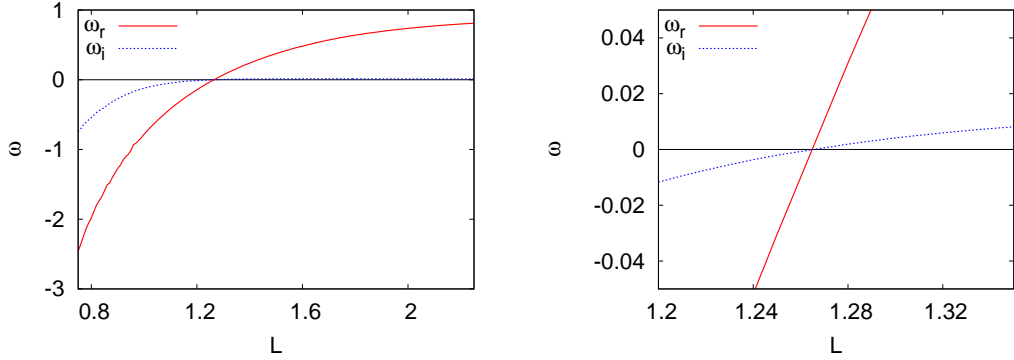


Figure 3: First mode frequencies (left) and near the transition (right). (color online)

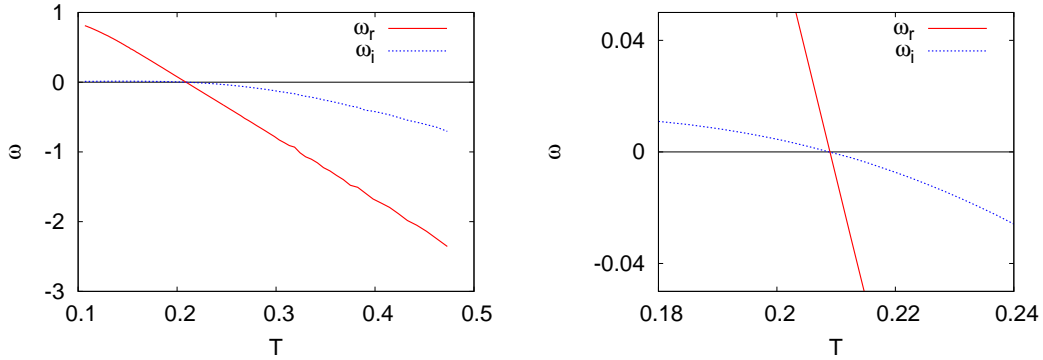


Figure 4: First mode frequencies in function of T (left) and near the transition (right). (color online)

The frequencies of the second mode displays a behaviour similar to the first mode. Again, choosing the sign of ω_r as the same of ω_i , we see that both frequencies change sign at the same point. These frequencies are shown in Figure (6).

In Figure (7) we have the comparison between the results obtained using two different numerical approaches: the finite difference method Eq.(13) and Horowitz-Hubeny method Eq.(23). The vertical line separates the stable and unstable regions.

In the stable region, the behavior of the real part of the quasinormal frequencies as L increases is quite similar in both approaches. However, after the phase transition, the Horowitz-Hubeny method gives a rather different result. A possible explanation for this

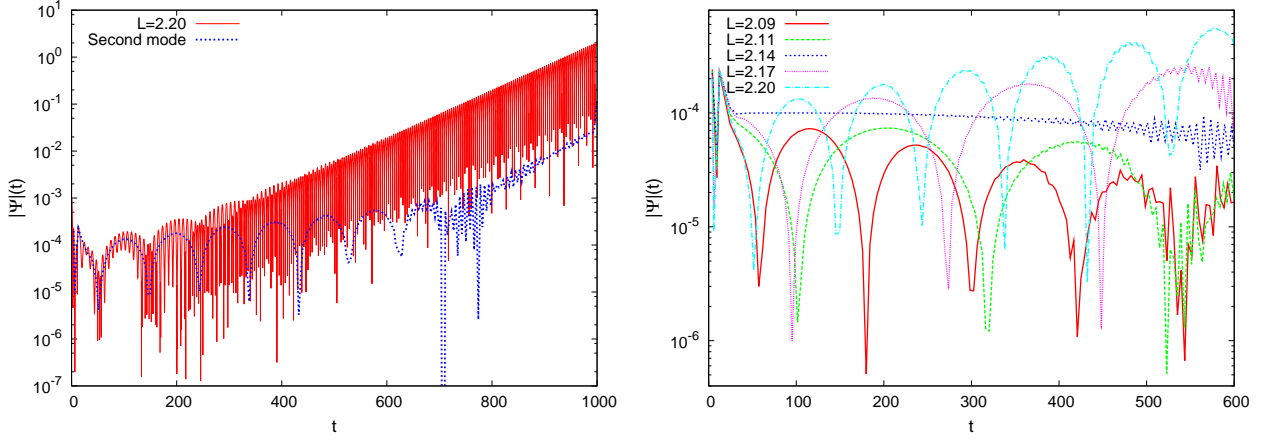


Figure 5: Evolution of $\Psi(t)$ with isolated second mode (left) and second mode behaviours for several L (right). (color online)

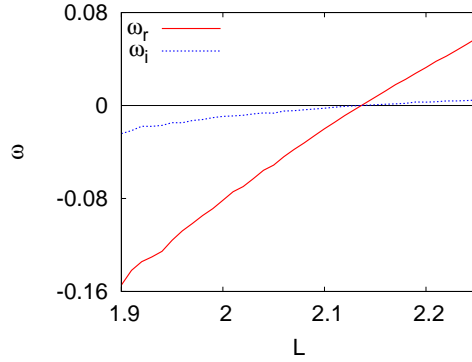


Figure 6: Second mode frequencies (color online).

behavior could be due to the fact that in the neighborhood of the phase transition point L_* , the real part of the frequencies computed through this method may be the frequencies of the second mode. Indeed, zero frequencies do not show up in the Horowitz-Hubeny method due to its limitations as already discussed in [15]. We also found some frequencies with positive imaginary part using the Horowitz-Hubeny method. However, it does not seem to converge as we increase the truncation order N . Therefore, we cannot rely on the results in this region.

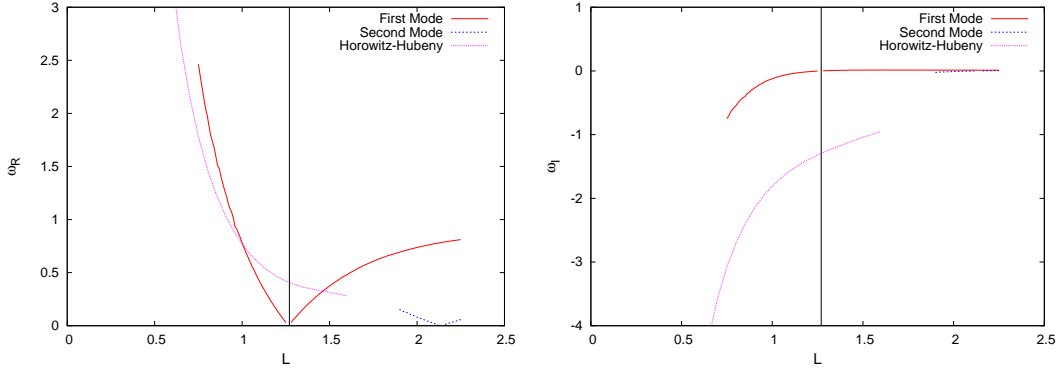


Figure 7: Comparison between real frequencies (left) and imaginary frequencies (right). (color online)

According to [19], polynomials with large terms (e.g. $\sim 10^{18}$) can be pathologic. A vanishingly small change in a very small term can drastically change the roots in such cases. In the Horowitz-Hubeny method, the larger the truncation order N , the larger the terms of the polynomial are. Thus, for sufficiently large values of N , even small numerical errors from polynomial calculation can lead to a completely different root. That explains why the roots stop converging after a certain N . In this work, the first derivative term in (10) implies in larger terms in the polynomial and the algorithm stops converging for N smaller than what is expected for systems with $q = 0$. The approximate positions of the zeros as well as stability are confirmed as well.

Therefore, we conclude that there are exactly two phases in the model, a stable phase for small values of L (normal phase) and a unstable superconducting phase for $L > 1.28$, or for temperatures $T < 0.21$. We expect such results and phase structure to remain true in other holographic models (as e.g. with different topologies).

Acknowledgments

This work has been supported by FAPESP (*Fundação de Amparo à Pesquisa do Estado de São Paulo*) and CNPq (*Conselho Nacional de Desenvolvimento Científico e Tecnológico*), Brazil.

-
- [1] J. Maldacena, *Adv. Theor. Math. Phys.* **2**, 231, (1998);
E. Witten, *Adv. Theor. Math. Phys.* **2**, 253, (1998).
- [2] G. Policastro, D. T. Son, A. O. Starinets, *Phys. Rev. Lett.* **87**, 081601, (2001).
- [3] G. Policastro, D. T. Son, A. O. Starinets, *JHEP*, **0209**, 043, (2002);
G. Policastro, D. T. Son, A. O. Starinets, *JHEP*, **0212**, 054, (2002);
D. T. Son, A. O. Starinets, *Ann. Rev. Nucl. Part. Sci.* **57**, 95, (2007).
- [4] S. S. Gubser *Phys. Rev.* **D78** , 065034, (2008).
- [5] Ruth Gregory, Sugumi Kanno, Jiro Soda, *JHEP* **0910**, 010, (2009);
Luke Barclay, Ruth Gregory, Sugumi Kanno, Paul Sutcliffe, hep-th 1009.1991, (2010).
- [6] Qiyuan Pan, Bin Wang, Eleftherios Papantonopoulos, J. Oliveira, A. B. Pavan, *Phys. Rev.* **D81** , 106007, (2010).
- [7] Xi He, Bin Wang, Rong-Gen Cai, Chi-Yong Lin, *Phys. Lett.* **B688** , 230, (2010).
- [8] K. Maeda, S. Fujii, *Phys. Rev.* **D81**, 124020, (2010).
- [9] Massimo Siano, arXiv:1010.0700v1 [hep-th]
- [10] Keiju Murata, Shunichiro Kinoshita, Norihiro Tanahashi, arXiv:1005.0633v1 [hep-th]
- [11] S. S. Gubser, *Class. Quant. Grav.* **22** , 5121, (2005).
- [12] Kostas D. Kokkotas, Bernd G. Schmidt, *Living Rev. Rel.* **2**, 2, (1999);
Emanuele Berti, Vitor Cardoso, Andrei O. Starinets, *Class. Quant. Grav.* **26**, 163001, (2009);
Bin Wang, *Braz. J. Phys.* **35**, 1029, (2005).
- [13] S. A. Hartnoll, C. P. Herzog and G. T. Horowitz, *Phys. Rev. Lett.* **101**, 031601 (2008).
- [14] B. Wang, C. Y. Lin and C. Molina, *Phys. Rev. D* **70**, 064025 (2004).
- [15] Gary T. Horowitz, Veronika E. Hubeny, *Phys. Rev.* **D62**, 024027, (2000).
- [16] B. Wang, C.Y. Lin, and E. Abdalla, *Phys. Lett. B* **481**, 79 (2000).
- [17] R. A. Konoplya, *Phys. Rev. D* **66**, 084007 (2002)
- [18] W. H. Press, S. A. Teukolsky, W. T. Vetterling, B. P. Flannery, *Numerical Recipes*, third edition, Cambridge University Press, Cambridge, (2007)
- [19] Forman S. Acton , *Numerical Methods that Work*, fourth printing, Mathematical Association of America, (1990)